



Brazilian Crude Oil Physicochemical Characterization and Its Rheology Below the Wax Appearance Temperature.

Flavio P. B. Lins Junior¹, Rafael M. Charin¹, Krishnaswamy Rajagopal^{1*}

¹Laboratório de Termodinâmica e Cinética Aplicada, Escola de Química, UFRJ, Brazil, *raja@eq.ufrj.br

Abstract

The apparent viscosity of five Brazilian crude oil samples from different Floating Production Storage and Offloading (FPSO) units from the Santos and Campos basins was measured at temperatures below the wax appearance temperature (WAT). Composition, molar mass, WAT and API gravity (°API) of the samples were determined to characterize the samples. It was found that most crude oils samples have two WATs in the range of 80°C to 4 °C with one exception. The samples present non-newtonian behavior when below the lower WAT that can be well described by the Carreau-Yasuda rheological model. Below the higher WAT and above the lower was identified a mixed Newtonian and non-Newtonian Behavior.

Keywords

crude oil; viscosity; rheology

Introduction

Rheology plays an important role in the oil and gas industry. Due to the chemical complexity of petroleum fluids, their rheological properties can vary from Newtonian to highly non-Newtonian behavior. When wax precipitates in the oil, a complex multi-phase system is formed that can exhibit pseudoplastic behavior and viscoelasticity, a behavior that's much harder to accurately model and characterize [1]. Crude oils with high wax content can present a flow assurance challenge during transient operations, such as production shutdowns, because wax will precipitate when the crude oil cools down. In this study, five samples of Brazilian crude oils from different origins were characterized, and their rheological behavior was measured using a rotational rheometer, producing experimental data that can be used to further understand the relationship between the crude oils' physical-chemical properties and their rheological behavior.

Methodology

Physicochemical Characterization

The compositions of the samples were measured by gas chromatography according to the ASTM D2887 standard. The °API was measured using an oscillatory tube densimeter according to the ASTM 5002-99 standard. The average molar mass of the crude oil was measured using a cryoscopy technique based on the freezing point depression of benzene in the presence of dissolved oil. The WAT was measured using differential scanning calorimetry (DSC) with a cooling rate of 1°C/min from 80°C to 4°C. The precipitated crystals were

observed under polarized visible light using a microscope with 50x magnification objective lenses, equipped with a digital camera and temperature control. The images were used for qualitative analysis only.

Rheometric Measurement

Before any measurements were performed, the samples were heated to 80°C for at least 30 minutes to dissolve any wax crystals initially present in the crude oil. The experiments were conducted using a TA Instruments Ares G2 rotational rheometer in a 40 mm diameter crosshatched plate-plate geometry with a 1 mm gap between the top and bottom parts of the measuring elements. This geometry was chosen to prevent wall slip, a common occurrence in particulate fluid systems, and to minimize the amount of sample used. The apparent viscosity of the crude oil samples was measured as a function of shear rate in the range from 0.01 s⁻¹ to 300 s⁻¹ at 4°C, 10°C, and 20°C or 30°C, obtaining 46 measurements for each viscosity curve. Measurements outside the equipment's accuracy range were discarded.

Results Analysis

For the samples with non-Newtonian behavior, the five parameter Carreau-Yasuda model [2], Eq. (1) was used to describe the obtained viscosity curves.

$$\eta(\dot{\gamma}) = \eta_{\infty} + (\eta_0 - \eta_{\infty}) (1 + (\lambda \dot{\gamma})^a)^{-(1-n)/a} \quad (1)$$

where $\eta(\dot{\gamma})$ [Pa.s] is the apparent viscosity of the fluid, η_{∞} [Pa.s] is the infinite shear rate viscosity, η_0 [Pa.s] is the zero shear rate viscosity, $\dot{\gamma}$ [s⁻¹] is

the shear rate, λ [s] is the time constant indicating relaxation time [s], n is the power law index [-], and a [-] is a parameter related to the transition from the Newtonian to the power law behavior. The parameters of the model were determined for each viscosity curve using the generalized reduced gradient optimization algorithm. The model fit to the experimental data was evaluated using the determination coefficient R^2 - Eq. (2), as statistical criteria.

$$R^2 = 1 - \frac{\sum^N (\eta_{\text{exp}} - \eta_{\text{mod}})^2}{\sum^N (\eta_{\text{exp}} - \eta_{\text{mean}})^2} \quad (2)$$

Results and Discussion

The compositions of the samples obtained by gas chromatography analysis are shown in Tab 1. The molar mass, WAT and °API of the samples are shown in Tab. 2.

Table 1. Sample Composition (%mol)

	C3-C6	C7-C12	C12-19	C20+
Sample 1	3.08	34.47	24.41	38.04
Sample 2	4.43	27.56	27.18	40.83
Sample 3	4.86	36.35	24.06	34.72
Sample 4	2.34	26.87	23.89	46.90
Sample 5	3.58	29.36	26.00	41.06

Table 2. Sample Physicochemical Properties

	MM (g/gmol)	WAT 1 (°C)	WAT 2 (°C)	°API
Sample 1	291.39	52.65	23.57	26.75
Sample 2	301.74	36.76	13.75	21.64
Sample 3	297.60	18.51	-	27.27
Sample 4	354.78	46.84	27.48	21.95
Sample 5	312.92	36.52	16.26	23.19

The samples consist of Medium and Heavy oils based on the °API measurements ranging from 21.64 to 27.27. The only sample to have one WAT in the analysis range is the sample 3. Figure 1 and Fig. 2 shows the DSC analysis for the WAT determination for the sample 1 and sample 3.

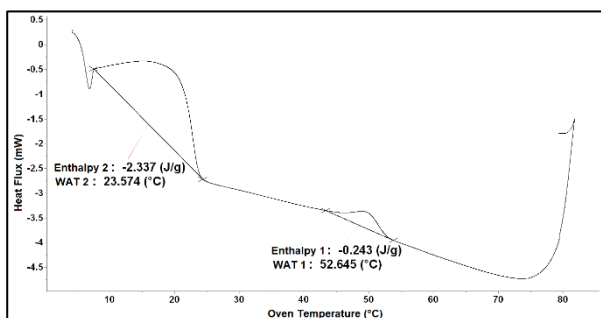


Figure 1: WAT determination for the sample 1

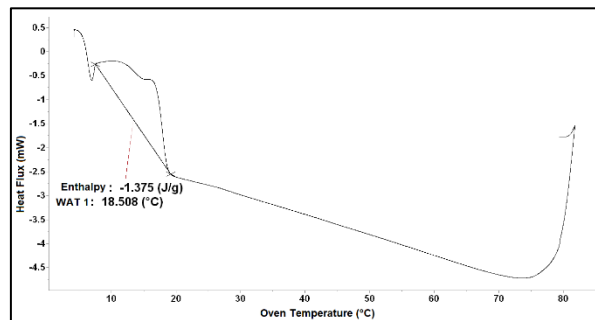


Figure 2. WAT determination for the sample 3.

Sample 1 and Sample 3 have similar average molar masses, °API, and compositions but different WATs. This demonstrates how small compositional differences can have a significant impact on wax precipitation. Figure 3 shows the viscosity curves for the samples below the lower WAT, and Figure 4 shows the curves for the samples between the two WATs.

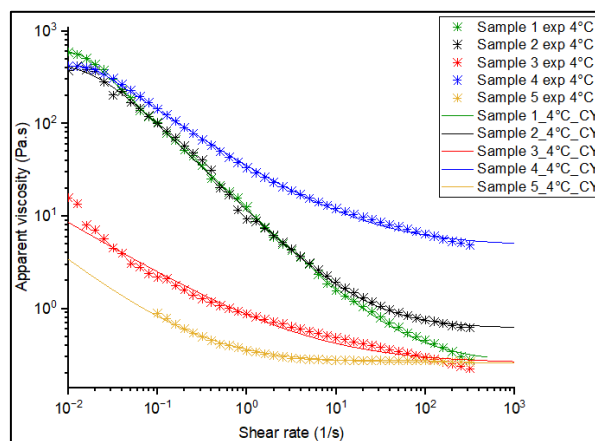


Figure 3. Apparent viscosity curves for the samples below the lower WAT.

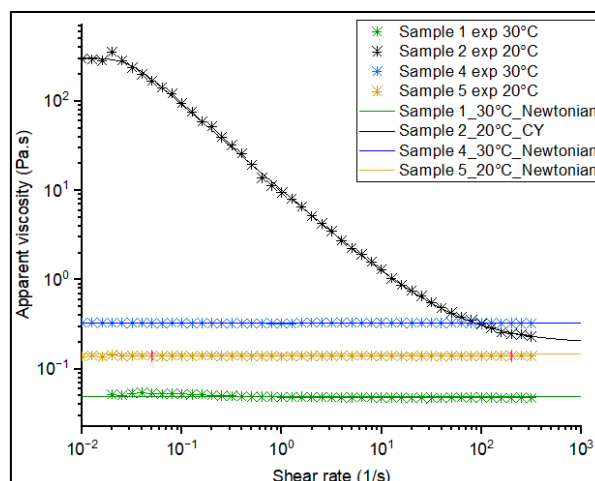


Figure 4. Apparent viscosity curves for the samples between the WATs.

All samples exhibit non-Newtonian pseudoplastic behavior when the system is below the lower WAT. Above the lower WAT and below the higher WAT, Samples 4, 5, and 1 exhibit Newtonian behavior, while Sample 2 is pseudoplastic. The experimental data is well described by the Carreau-Yasuda

rheological model. Tables 3–7 show the regression parameters obtained for Samples 1–5. The lowest coefficient of determination obtained was $R^2 = 0.9307$ for Sample 3 at 4°C.

Table 3. Parameters of Carreau-Yasuda model for sample 1.

	Sample 1 (4°C)	Sample 1 (10°C)	Sample 1 (20°C)
η_0 (Pa.S)	587.281	997.9280	20.5188
η_∞ (Pa.S)	0.2636	0.1640	0.0685
λ (s)	69.5329	139.3020	209.5210
n	0.0780	0.0448	0.1812
a	7.0917	0.7284	12.2322
R^2	0.9995	0.9996	0.9974

Table 4. Parameters of Carreau-Yasuda model for sample 2.

	Sample 2 (4°C)	Sample 2 (10°C)	Sample 2 (20°C)
η_0 (Pa.S)	476.7890	310.3880	300.7950
η_∞ (Pa.S)	0.6131	0.3625	0.1964
λ (s)	50.7922	57.4396	33.6833
n	0.0448	0.0616	0.0309
a	1.7573	1.8163	3.4912
R^2	0.9986	0.9999	0.9997

Table 5. Parameters of Carreau-Yasuda model for sample 3.

	Sample 3 (4°C)	Sample 3 (10°C)	Sample 3 (20°C)
η_0 (Pa.S)	36.0608	10.8423	1.3988
η_∞ (Pa.S)	0.2818	0.1428	0.0348
λ (s)	802.7210	173.0753	276.1180
n	0.3811	0.1465	0.0397
a	7.2144	1.8251	2.0239
R^2	0.9307	0.9985	0.9986

Table 6. Parameters of Carreau-Yasuda model for sample 4.

	Sample 4 (4°C)	Sample 4 (10°C)
η_0 (Pa.S)	388.2140	376.8922
η_∞ (Pa.S)	4.6810	2.3566
λ (s)	49.1784	239.0631
n	0.3509	0.3924
a	18.7889	2.5172
R^2	0.9986	0.9994

Table 7. Parameters of Carreau-Yasuda model for sample 5.

	Sample 5 (4°C)	Sample 5 (10°C)
η_0 (Pa.S)	17.1519	0.8390
η_∞ (Pa.S)	0.2749	0.1650
λ (s)	385.1003	298.9021
n	0.0930	0.5243
a	2.0057	4.9807
R^2	0.9752	0.9828

η_0 (Pa.S)	17.1519	0.8390
η_∞ (Pa.S)	0.2749	0.1650
λ (s)	385.1003	298.9021
n	0.0930	0.5243
a	2.0057	4.9807
R^2	0.9752	0.9828

Sample 1 at 30°C, Sample 4 at 30°C, and Sample 5 at 20°C behave as Newtonian fluids with viscosities of 0.0482 Pa·s, 0.3245 Pa·s, and 0.1463 Pa·s, respectively. Figure 5 shows the microscopy for Sample 5 at 20°C, and Figure 6 shows the same sample at 10°C. It can be seen that when the system is at 20°C, above the lower WAT and below the higher WAT, fewer crystals form, which may explain why the system exhibits Newtonian behavior at this condition but not at 10°C, when a higher number of crystals is present.

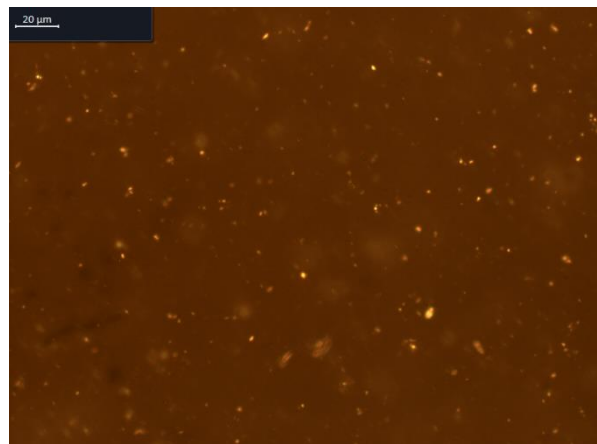


Figure 5. Polarized light microscopy for sample 5 at 20°C

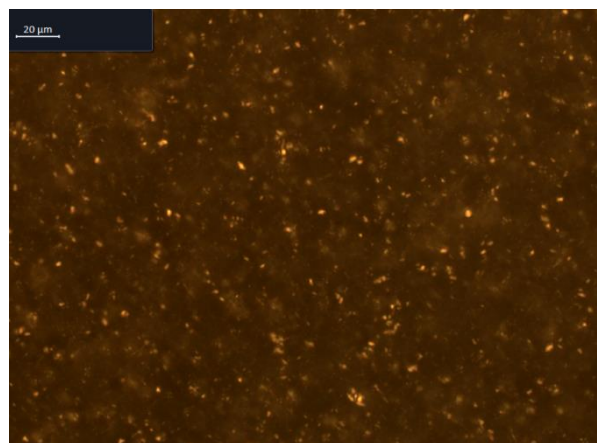


Figure 6. Polarized light microscopy for sample 5 at 10°C

Conclusions

Five medium and heavy crude oil samples from Brazilian oil fields were characterized by their physicochemical and rheological properties. Across the temperature range from 80°C to 4°C, the samples exhibited two wax appearance temperatures, except for Sample 3. At temperatures below the lower WAT, all samples

show pseudoplastic behavior; at temperatures between the two WATs, the crude oils can behave as either Newtonian or non-Newtonian. The pseudoplastic behavior of the samples can be well described by the Carreau-Yasuda rheological model. Images obtained by polarized light microscopy showed that the system has more precipitated wax crystals at temperatures below the lower WAT, which explains the deviation from Newtonian behavior. The experimental data produced can be used to further understand the relationships between the physicochemical and rheological properties of crude oils.

Acknowledgments

The authors would like to thank professor Verônica Calado for the support with the Rheological analysis. Professor Marcio Nele de Souza and André da Silva Guimarães for the support with the use of the microscope and the LMCP lab team for the DSC analysis.

Responsibility Notice

The authors declare that they are solely responsible for all information in this paper.

References

- [1] Rønningsen, H.P; *Rheology of petroleum fluids*. ATNRS 20, 11-18, 2012
- [2] Wozniak, M. *et al. Some rheological properties of plastic greases by Carreau-Yasuda model*. *Trib. Int.*, v. 183, p.108372, Coimbra, 2023.